Magnetic characterization and modeling of FeMn/Co/Ru/Co artificial antiferromagnets

G. J. Strijkers, S. M. Zhou, F. Y. Yang, and C. L. Chien
Department of Physics and Astronomy, The Johns Hopkins University, Baltimore, Maryland 21218
(Received 5 July 2000)

FeMn/Co/Ru/Co artificial antiferromagnets for use in giant magnetoresistive spin-valve elements were fabricated and magnetically characterized. The magnetization behavior of the films can be understood by coherent rotation of the magnetizations of the layers. A simple model is presented which reproduces all the basic characteristics of the magnetization loops, e.g., shape, switching fields, and magnitude of the pinning field as a function of thickness. The model is also extended to a complete spin-valve system, including the effects of coupling between the biased layer and the free layer.

In recent years a number of different spin-valve structures have been introduced to apply the giant magnetoresistance (GMR) effect in magnetic sensors.[1] The most successful scheme consists of a spin-valve biased by a so-called artificial (or synthetic) antiferromagnet,[2–4] such as FeMn/Co/Ru/Co. In this structure the sensitivity of an exchange biased system is combined with the magnetic rigidity of the interlayer exchange coupled system. The characteristics of an artificial antiferromagnet depend sensitively on the thickness of the two ferromagnetic layers.

In this paper we present measurements of the FeMn/Co/Ru/Co bias system to obtain characteristics of the magnetization behavior of this system. A simple model calculation assuming coherent rotation of the magnetizations is able to explain the basic features of the magnetization loops, e.g., switching fields and magnitude of the pinning field as a function of thickness. The calculations are also extended to a complete spin-valve system, including a free layer to model the effects of ferromagnetic coupling (orange-peel coupling, interlayer exchange) between the biased layer and the free layer.

The multilayers of 100 Å FeMn/60 Å Co/7 Å Ru/t_{Co} Co, with t_{Co} ranging from 10 to 100 Å, were prepared onto Si substrates by dc magnetron sputtering at 6 mTorr Ar pressure in a multisource deposition chamber with a base pressure better than 1×10^{-7} Torr. A Cu seed layer ensures that the layers are predominantly (111) textured as was established by x-ray diffraction measurements, and a Cu capping layer protects the structure from oxidation. Exchange biasing was induced by cooling the sample from 420 K in a field of 10 kOe (in the same direction as the positive field of all the magnetization curves presented in this paper). Magnetization measurements were performed at room temperature in a vibrating sample magnetometer.

Figure 1(a) shows the magnetization loop for a top Co layer thickness $t_{\mathrm{Co}}=88$ Å, representative for all other samples. Starting from a large negative field, the magnetic moments begin to rotate at about -1900 Oe towards a plateau with an antiparallel orientation of the magnetizations. The magnetization curve is not symmetrical with respect to zero field. At positive fields a jump at about 130 Oe and then a rotation towards saturation at about 1800 Oe is observed. Details of this magnetization loop can be understood by a simple model assuming only rotation of the magnetic moments. This simplification is justified because of the strong antiferromagnetic coupling between the two Co layers, which favors a rotation of the magnetic moments rather than a reversal mechanism with domain wall nucleation and propagation, as is observed in exchange-biased layers.[5] From an application point of view rotation of the magnetic moments is more desirable because domain wall nucleation and movement leads to a larger hysteresis. Indeed spin valves based on artificial antiferromagnets display much smaller hysteresis than exchange biased spin valves.[3,6,7]

To calculate the magnetization loop we consider the areal energy density of the stack of layers

$$E=-M_1H\cos\phi_1-M_2H\cos\phi_2-J_1\cos(\phi_1-\phi_2)-J_{\mathrm{eb}}\cos\phi_1. \quad (1)$$

Here M_1 and M_2 are the magnetic moments of the bottom and the top Co layer, respectively, and ϕ_1 and ϕ_2 are the

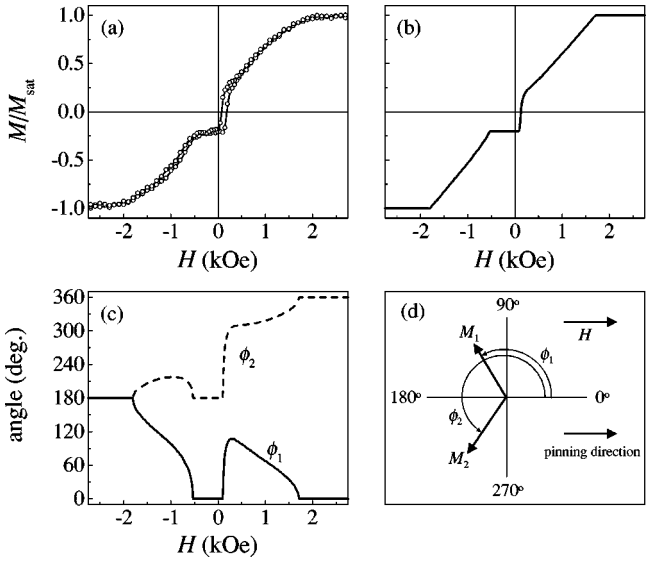

FIG. 1. (a) Normalized magnetization curve at room temperature of 100 Å FeMn/60 Å Co/7 Å Ru/88 Å Co. (b) Calculation of the magnetization curve with Eq. (1). (c) Variation of the angle of the bottom (ϕ_1) and the top (ϕ_2) Co layer as function of the applied field. (d) Definition of the angles with respect to the applied field H and the pinning direction of the bottom Co layer.

angles of the magnetic moments with respect to the applied field H [see Fig. 1(d)]. J_1 is the interlayer exchange coupling energy between the two Co layers (<0 for antiferromagnetic coupling) and J_{eb} is the exchange biasing energy between the FeMn and the bottom Co layer. The crystalline anisotropy for these (111) textured sputtered Co layers is small and is therefore neglected.

The measured magnetization loops are well reproduced by minimizing Eq. (1) with respect ϕ_1 and ϕ_2 as functions of the applied fields H, as demonstrated in Fig. 1(b). The fitting parameters are the interlayer exchange coupling J_1 between the two Co layers and the exchange biasing energy J_{eb} between the FeMn and the bottom Co layer. The fit for this particular stack of layers resulted in $J_1=-0.9$ erg/cm^2 and $J_{eb}=0.065$ erg/cm^2, in good agreement with coupling strengths reported in literature.[8,9]

The details of the magnetization reversal can now be understood in more detail from Fig. 1(c), which shows the variation of the angles of the bottom and the top Co layer as a function of the applied field. The definition of ϕ_1 and ϕ_2 is shown in Fig. 1(d). Starting from saturation at high negative field, first the bottom Co layer rotates 180° towards an antiparallel orientation with respect to the top Co layer and the magnetic field H. During this reversal the top Co layer tilts away about 40° from its equilibrium direction along the field due to the strong antiferromagnetic coupling with the bottom Co layer. At a positive field of about 130 Oe a fast rotation occurs in which both layers tilt away about 100° from the field direction. However, the relative antiparallel orientation of the two magnetic moments is nearly maintained. When the field is further increased the antiferromagnetic coupling is overcome and the two moments finally align parallel to the field at about 1700 Oe.

Figure 2 shows the measured magnetization curves (left-hand side) for a thickness of the top Co layer $t_{Co}=18$, 60, and 95 Å with corresponding fits (right-hand side). When the top Co layer thickness is thinner than the exchange biased Co layer [Figs. 2(a) and 2(b)], the total magnetization crosses zero at a negative field. On the other hand when the top Co layer is thicker than the exchange biased Co layer [Figs. 2(e) and 2(f)], the total magnetization crosses zero at positive field. This has recently been exploited by Marrows *et al.*[4] to create a bridge sensor in which two of the spin-valve elements have a negative response and two a positive response upon the application of a field.

The most favorable characteristics are obtained, however, when both magnetic layers are equal in thickness, the so-called balanced configuration, as shown in Figs. 2(c) and 2(d). Not only are stray fields from the artificial antiferromagnet minimal for this balanced structure, but also the field range for which the two magnetic layers are antiparallel is maximal in positive and negative field directions. This is illustrated in Fig. 3(a), in which the measured pinning field H_{pin} (defined as the field where the magnetization crosses or approaches zero in the middle of the hysteresis) is plotted as a function of the top Co layer thickness. Figure 3(a) is supplemented with a calculation, based on Eq. (1), of the pinning field with $J_1=-0.9$ erg/cm^2 and $J_{eb}=0.065$ erg/cm^2.

In an actual spin-valve element the magnitude of the pinning fields can be enhanced by optimizing the Ru thickness to increase the antiferromagnetic coupling, or by reducing the magnetic layer thicknesses as is demonstrated in Fig. 3(b). This figure shows a calculation of the evolution of the positive and negative pinning fields, H_1 and H_2 [see Fig. 2(d)], for the balanced structure 100 Å FeMn/t_{Co} Co/7 ÅRu/t_{Co} Co as function of t_{Co}. Antiferromagnetic coupling strength and exchange biasing coupling strength are the same as for Fig. 3(a).

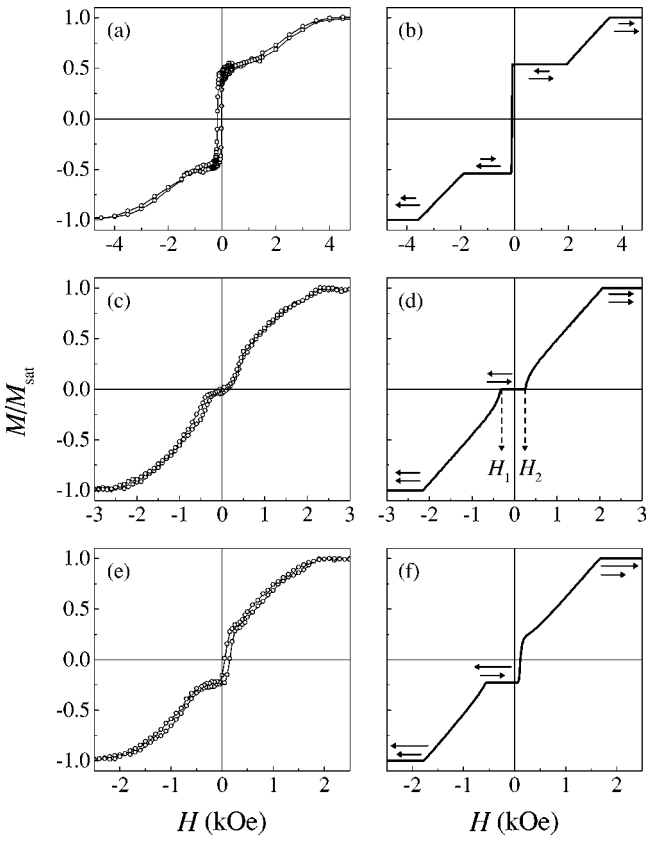

FIG. 2. Normalized measured (left-hand side) and calculated (right-hand side) magnetization loops of 100 FeMn/60 Å Co/7 Å Ru/t_{Co} Co, with t_{Co} [(a),(b)] 18 Å, [(c),(d)] 60 Å, and [(e),(d)] 95 Å. The solid arrows indicate the orientations of the magnetic moments of the two Co layers at several fields.

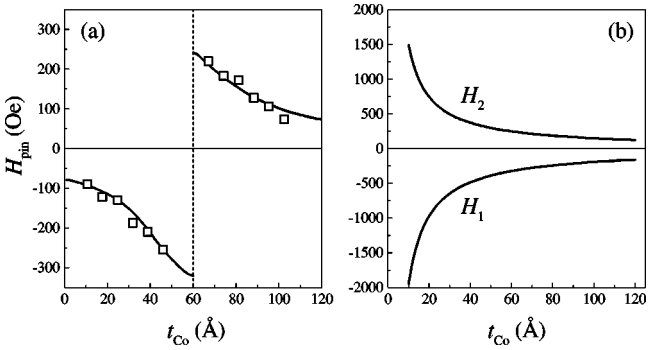

FIG. 3. (a) Measured (squares) and calculated pinning field (solid line) for 100 Å FeMn/60 Å Co/7 Å Ru/t_{Co} Co as function of t_{Co}. (b) Calculated pinning fields for the balanced structure 100 Å FeMn/t_{Co} Co/7 Å Ru/t_{Co} Co as function of t_{Co}. H_1 and H_2 are defined as shown in Fig. 2(d).

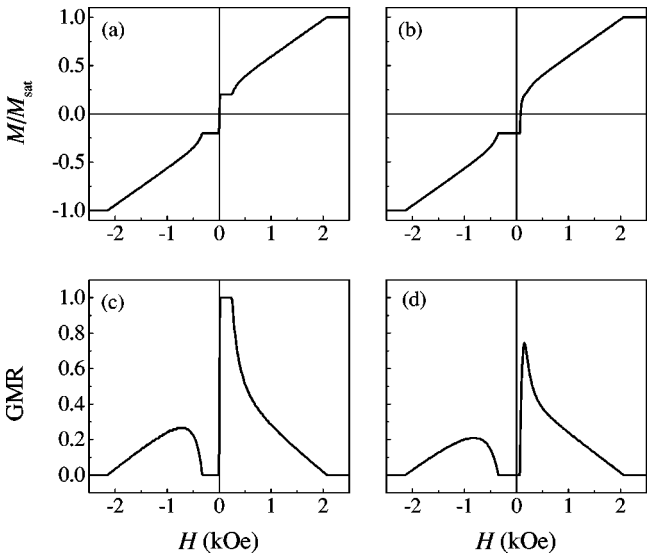

FIG. 4. Calculation of the magnetization loop and the normalized magnetoresistance curve of the full spin-valve system 100 Å FeMn/60 Å Co/7 Å Ru/60 Å Co/NM/30 Å $Ni_{80}Fe_{20}$, with [(a),(c)] $J_f=0$, and [(b),(d)] $J_f=0.02$ erg/cm^2. The magnetoresistance is defined as GMR$=[1-\cos(\phi_2-\phi_3)]/2$.

Finally, we have extended the model calculations to a complete spin-valve system of the following composition: 100 Å FeMn/60 Å Co/7 Å Ru/60 Å Co/NM/30 Å $Ni_{80}Fe_{20}$, with NM a nonmagnetic layer (for example Cu). The areal energy density of this system now includes a third magnetic layer and reads

$$E=-M_1H\cos\phi_1-M_2H\cos\phi_2-M_3H\cos\phi_3-J_1\times\cos(\phi_1-\phi_2)-J_{eb}\cos\phi_1-J_f\cos(\phi_2-\phi_3), \quad (2)$$

which also includes an interlayer exchange coupling constant J_f between the ''free'' $Ni_{80}Fe_{20}$ layer and the top Co layer to account for any coupling between the free layer and the top Co layer. The origin of J_f is for example orange-peel coupling or some ferromagnetic interlayer exchange coupling between the two layers ($J_f>0$). As before, the magnetization and magnetoresistance curves are calculated by minimizing Eq. (2) with respect to ϕ_1, ϕ_2, and ϕ_3 as function of the applied field H.

Figures 4(a) and 4(c) show the calculated normalized magnetization loop of the complete spin-valve and the corresponding normalized magnetoresistance curve for the case of no exchange coupling between the free $Ni_{80}Fe_{20}$ layer and the top Co layer. The free layer switches exactly at zero field because it has no interaction with the other layers, and therefore a full antiparallel situation is reached at positive fields leading to a maximal magnetoresistance GMR$=1$.

Ferromagnetic coupling due to, for example, correlated roughness (orange-peel coupling) is a known problem for the control of the magnetic response of spin-valves systems.[10,11] To demonstrate the effect of ferromagnetic coupling Figs. 4(b) and 4(d) show the calculated magnetization curve and magnetoresistance loop for a ferromagnetic coupling constant $J_f=0.02$ erg/cm^2, which is of the correct order of magnitude for some spin-valve systems.[10–12] As clearly can be seen, the plateau in the magnetization loop at positive fields has disappeared, indicating an incomplete antiparallel alignment of the magnetic layers, which is also reflected in a reduced GMR. Furthermore the switching field is shifted from zero field to about 60 Oe and extends over approximately 90 Oe, reducing the sensitivity of the spin-valve structure dramatically.

In conclusion we have presented systematic measurements and analysis of FeMn/Co/Ru/Co artificial antiferromagnetic layers. A simple model was introduced which is able to account for all the basic characteristics of the magnetization loops, e.g., shape, switching fields and magnitude of the pinning field as a function of thickness. We have extended the calculations to a complete spin-valve system to include the effects of ferromagnetic coupling between the bias system and the free layer of the spin valve. A reduced GMR was found as a result of an incomplete antiparallel alignment of the magnetic layers.

This work was supported by NSF Grant No. DMR96-32526.

[1] See e.g., J. M. Daughton, J. Magn. Magn. Mater. **192**, 334 (1999).
[2] D. Heim and S. S. P. Parkin, US Patent No. 5,465,185.
[3] K.-M. H. Lenssen, A. E. T. Kuiper, and F. Roozeboom, J. Appl. Phys. **85**, 5531 (1999).
[4] C. H. Marrows, F. E. Stanley, and B. J. Hickey, Appl. Phys. Lett. **75**, 3847 (1999).
[5] V. I. Nikitenko, V. S. Gornakov, A. J. Shapiro, R. D. Shull, K. Liu, S. M. Zhou, and C. L. Chien, Phys. Rev. Lett. **84**, 765 (2000).
[6] M. Saito, N. Hasegawa, F. Koike, and H. Seki, J. Appl. Phys. **85**, 4928 (1999).
[7] M. Mao, M. Miller, P. Johnson, H. C. Tong, C. Qian, L. Miloslavsky, C. Y. Hung, J. Wang, and H. Hegde, J. Appl. Phys. **85**, 4454 (1999).
[8] P. J. H. Bloemen, H. W. van Kesteren, H. J. M. Swagten, and W. J. M. de Jonge, Phys. Rev. B **50**, 13 505 (1994).
[9] J. Nogues and I. K. Schuller, J. Magn. Magn. Mater. **192**, 203 (1999).
[10] Th. G. S. M. Rijks, R. F. O. Reneerkens, R. Coehoorn, J. C. S. Kools, M. F. Gillies, J. N. Chapman, and W. J. M. de Jonge, J. Appl. Phys. **82**, 3442 (1997).
[11] J. C. S. Kools, W. Kula, D. Mauri, and T. Lin, J. Appl. Phys. **85**, 4466 (1999).
[12] D. C. Parks, P. J. Chen, W. F. Egelhoff, Jr., and R. D. Gomez, J. Appl. Phys. **87**, 3023 (2000).